THE ASTROPHYSICAL JOURNAL, 454:862–871, 1995 December 1

THE CIRCUMSTELLAR MOLECULAR CORE AROUND L1551 IRS 5

G. A. FULLER[1]
National Radio Astronomy Observatory,[2] 949 N. Cherry Avenue, Campus Building 65, Tucson, AZ 85721
E. F. LADD[3]
Institute for Astronomy, University of Hawaii, 2680 Woodlawn Drive, Honolulu, HI 96822
R. PADMAN
Mullard Radio Astronomy Observatory, Cavendish Laboratory, Madingley Road, Cambridge, CB3 0HE, UK
P. C. MYERS
Harvard-Smithsonian Center for Astrophysics, 60 Garden Street, Cambridge, MA 02138
AND
FRED C. ADAMS
Department of Physics, University of Michigan, Ann Arbor, MI 48109
Received 1994 July 25; accepted 1995 June 8

ABSTRACT

We present maps of $C^{18}O$ and $C^{17}O$ $J = 2 \rightarrow 1$ emission toward the embedded young star L1551 IRS 5. The $C^{17}O$ emission traces a compact region $\sim$1900 AU in radius which is centered on the star which contains $\sim 0.1\ M_\odot$ of material. The integrated $C^{17}O$ emission has a crosslike structure aligned in the cardinal directions which is very similar to the structure seen in the submillimeter continuum emission from this source. A spatially more extended component of material which contains an additional 0.1 $M_\odot$ of material within 20″ of IRS 5, also contributes to the $C^{17}O$ emission. The cross gas is warmer and has a larger velocity dispersion than the more extended gas. The motions of the extended material imply a virial mass of 1–3 $M_\odot$, which is dominated by the mass of the central star plus disk. The $C^{18}O$ lines have considerable line wing emission and part of the cross is evident in this wing emission. Comparison with existing maps of the outflow near IRS 5 suggests that the cross material is part of the heated wall of the cavity evacuated by the outflow. The presence of such structures near embedded stars complicates the search for accreting material. However, the properties of the extended $C^{17}O$ emission constrain the mass accretion rate in L1551 IRS 5 to be less than $1.4 \times 10^{-5}\ M_\odot\ \mathrm{yr}^{-1}$. Comparison with the observed mass outflow rate from IRS 5 at a similar size scale suggests that there is currently little or no net accretion of material from the larger scale dense core into the central 2000 AU radius region about IRS 5.

Subject headings: circumstellar matter — ISM: jets and outflows — stars: individual (L1551 IRS 5) — star: pre–main-sequence

1. INTRODUCTION

The dense gas at the 0.1 pc size scale in nearby molecular clouds has been extensively studied (e.g., see reviews by Fuller 1993 and Myers 1994) and the association of obscured young stars with this gas has established that these regions are intimately involved in the star formation process (Beichman et al. 1986; Myers et al. 1987). However, the properties of the circumstellar material around young stars, which is the material most closely associated with the star formation process, are still poorly understood.

The strong far-infrared and submillimeter continuum emission from young stars clearly indicates that there is a significant amount of material very close to the stars (e.g., Cabrit & André 1991; Ladd et al. 1991; Terebey, Chandler, & André 1993), but the study of this material has been limited by the small size of these regions and the lack of a suitable molecular probe with which to study them. There are two motivations for studying this circumstellar material with molecular tracers. Molecular probes provide a determination of the column density and temperature of the circumstellar material which is independent of uncertain dust properties, such as the dust opacity. More importantly, spectroscopic studies directly probe the kinematics of the circumstellar region and provide a virial mass estimate.

Young stars are thought to have spatially separated but concurrent outflow of material driven by stellar winds, and infall of material (Parker, Padman, & Scott 1991; Terebey, Shu, & Cassen 1984). It is therefore desirable that a molecular probe of circumstellar material trace a region which is sufficiently spatially resolved that the effects of these two competing processes can be identified.

Rare isotopomers of chemically stable species are likely candidates for studying these circumstellar regions. These species are less likely than more reactive ones to suffer extreme chemical effects, for example, in regions where stellar winds impact the circumstellar material. Also, the lines of sufficiently rare species are optically thin in all but the densest regions close to the young star.

[1] Present address: National Radio Astronomy Observatory, 520 Edgemont Road, Charlottesville, VA 22903.

[2] Operated by Associated Universities, Inc., under cooperative agreement with the National Science Foundation.

[3] Present address: Five College Radio Astronomy Observatory, 619 Lederle Graduate Research Center, University of Massachusetts, Amherst, MA 01003.

In this paper we report the first results of a study of rare forms of carbon monoxide toward the circumstellar regions of young stars. We represent recent observations of the $J = 2 \rightarrow 1$ emission of $C^{17}O$ and $C^{18}O$ with 20″ angular resolution toward the well-known young star L1551 IRS 5. $C^{17}O$ is about 3.5 times less abundant than the more commonly studied rare isotopomer of CO, $C^{18}O$ (Wilson, Langer, & Goldmith 1981) and is more than 10^3 times less abundant than the commonest form, ^{12}CO.

L1551 IRS 5 (Strom, Strom, & Vrba 1976) is a well studied, embedded young star in Taurus at distance of 140 pc (Elias 1978). It is optically invisible and modeling of its spectral energy distribution suggests that it is an embedded protostar still accreting material (Adams, Lada, & Shu 1987; Kenyon, Calvet, & Hartmann 1993a; Kenyon et al. 1993b). IRS 5 has a total luminosity of $\sim 30\ L_\odot$ (Cohen et al. 1984) and drives a bipolar outflow which extends to a total of $\sim 25'$ in the direction $\sim 45°$ east of north (Snell, Loren, & Plambeck 1980; Moriarty-Schieven & Snell 1988).

The submillimeter continuum emission from L1551 IRS 5 at 1100 μm, 850 μm, and 730 μm has recently been studied by Ladd et al. (1995). Using JCMT observations they find that in additional to an unresolved point source component associated with the central star, there is significant extended emission at each wavelength. At 1100 μm the extended emission is elongated in the north–south direction. The maps at the shorter wavelengths, and especially the 730 μm map, show the emission to have a crosslike distribution with the arms of the cross oriented in the north–south and east–west directions. Ladd et al. modeled the extended emission as arising from two components centered on IRS 5: an extended component modeled as a cool, smoothly distributed envelope and a compact component comprising a north–south, east–west cross of warmer material.

In this paper new observations of $J = 2 \rightarrow 1$ transition of $C^{17}O$ and $C^{18}O$ are discussed in § 2. In § 3 the structure of the $C^{17}O$ and $C^{18}O$ maps and line profiles are discussed. The physical parameters of the emitting material are derived in § 4. We consider the nature and origin of the circumstellar structure and the mass accretion rate near IRS 5 in § 5 and our main conclusions are presented in § 6.

2. OBSERVATIONS

Observations of the $J = 2 \rightarrow 1$ transition of $C^{17}O$ at 224.7 GHz toward L1551 IRS 5 were conducted with the James Clerk Maxwell Telescope (JCMT)[4] in Hawaii in 1992 December and 1993 March. A 5×5 grid with 10″ spacing centered on L1551 IRS 5 was observed on each occasion. These two maps were then combined to produce a final $C^{17}O$ map. The typical rms noise in the spectra from the combined map is 0.07 K. The full width half-maximum (FWHM) beam size of the JCMT at the frequency of the $C^{17}O$ is 21″ and the system temperature during the observing sessions was between 300 and 600 K. During the observations the telescope pointing was checked regularly and was found to have an uncertainty of about 5″.

$C^{18}O$ $J = 2 \rightarrow 1$ emission was mapped with the same telescope in 1993 September over the same region as the $C^{17}O$ with the same sampling. In addition, the $C^{18}O$ map was extended over a region $\pm 40''$ from IRS 5 with full-beam (i.e., 20″) spaced observations. The typical rms noise in the spectra from the $C^{18}O$ map is 0.13 K. During this observing session additional $C^{17}O$ $J = 2 \rightarrow 1$ spectra toward IRS 5 were also obtained. The system temperature during this observing session was around 300 K and regular checks on the telescope pointing showed it has an uncertainty of about 5″. All the observations at JCMT were made using beam switching. For the $C^{17}O$ observations a beam separation of 150″ was used while a 300″ beam separation was used the $C^{18}O$ observations.

The JCMT facility acousto-optical spectrometer (AOS-C) was used for the observations obtained in 1992 December and 1993 March. This spectrometer has a channel spacing of 0.33 km s^{-1} at the frequency of the $C^{17}O$ transition. During the 1993 September observations the JCMT "Dutch" autocorrelator spectrometer (DAS) was used in a configuration which has a channel separation of 0.10 km s^{-1} at the frequency of the $C^{17}O$ $J = 2 \rightarrow 1$ transition. However, the JCMT 230 GHz receiver system is not phase-locked, so variations in the local oscillator frequency contribute a velocity smearing to the observed spectra. This results in an effective velocity resolution of 0.5 km s^{-1} for both the AOS-C and DAS observations (P. Friberg, private communication).

A fit to the hyperfine structure of the AOS-C $C^{17}O$ data toward IRS 5 indicates that the $C^{17}O$ is well fitted by a single component with a Gaussian velocity distribution with a FWHM of 1.1 ± 0.1 km s^{-1}. This is somewhat larger than the 0.86 ± 0.03 km s^{-1} measured from the DAS data. Since the $C^{17}O$ map was made using AOS-C, all further reference to velocity widths of the $C^{17}O$ will refer to the fits to the AOS-C data, except where indicated, but it should be noted that these may somewhat overestimate the true velocity widths.

Additional observations were obtained in 1993 March and October at the California Institute of Technology Submillimeter Observatory (CSO)[5] using the facility acousto-optical spectrometer (AOS) with a channel spacing of 0.06 km s^{-1} and a resolution of approximately 0.2 km s^{-1}. In 1993 March, low-sensitivity maps extending $\pm 60''$ from L1551 IRS 5 in the $J = 2 \rightarrow 1$ lines of $C^{17}O$ and $C^{18}O$ were made. In 1993 October, spectra were obtained toward IRS 5 in the $J = 2 \rightarrow 1$ and $J = 3 \rightarrow 2$ transitions of $C^{17}O$ and the $J = 2 \rightarrow 1$ transition of $C^{18}O$. At the frequency of the $J = 3 \rightarrow 2$ transition the CSO has the same beam size as the JCMT at the $J = 2 \rightarrow 1$ transition.

3. RESULTS

3.1. *Spectra toward IRS 5*

Figure 1 shows the $J = 2 \rightarrow 1$ $C^{18}O$ spectrum together with those of $C^{17}O$ $J = 2 \rightarrow 1$ and $J = 3 \rightarrow 2$ toward IRS 5. The $C^{18}O$ line toward IRS 5 is well fitted by two Gaussian components: a "spike" with a width of 0.74 km s^{-1} at 6.17 km s^{-1} and a "broad" component with a width of 2.6 km s^{-1} centered at 6.32 km s^{-1}. The large width of the broad component and its spatial structure (§ 3.3.1) indicate that this component is real and is not an instrumental effect due to the local oscillator.

The $C^{17}O$ spectra were fitted for the total optical depth of the transition, the velocity of the line, the intrinsic velocity dispersion, and the line amplitude following the method described by Fuller & Myers (1993). The velocity separation of

[4] The James Clerk Maxwell Telescope is operated by the Royal Observatories on behalf of the Particle Physics and Astronomy Research Council of the United Kingdom, the Netherlands Organization for Scientific Research, and the National Research Council of Canada.

[5] The California Institute of Technology Submillimeter Observatory is operated by the California Institute of Technology under funding from the National Science Foundation.

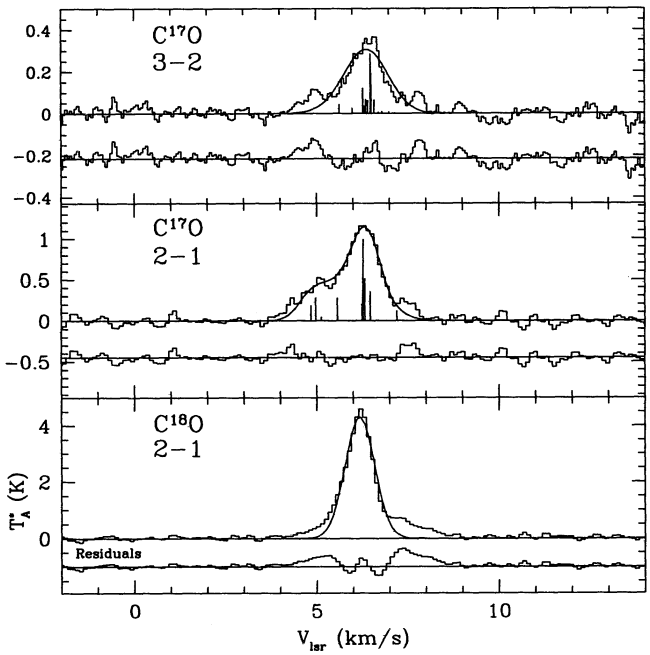

FIG. 1.—The spectra of $C^{18}O$ $J = 2 \rightarrow 1$ (*bottom*), $C^{17}O$ $J = 2 \rightarrow 1$ (*middle*) from JCMT using the DAS and $J = 3 \rightarrow 2$ (*top*) from CSO toward L1551 IRS 5. The solid curves through the spectra are single-velocity component fits and the residuals from the fit are shown below the spectrum in each panel. For the $C^{17}O$ transitions, the hyperfine structure of the transition is shown. For the $C^{18}O$ spectra, where the line wings are very apparent, the single component was fitted to the line core. The residuals for the $C^{17}O$ $J = 3 \rightarrow 2$ and $C^{18}O$ $J = 2 \rightarrow 1$ transitions clearly show the presence of a second, broader velocity component. The residuals for the $C^{17}O$ $J = 2 \rightarrow 1$ also suggest the presence of such a component.

the hyperfine components of the $C^{17}O$ transitions used in fitting the data were calculated using the coupling constants determined by Frerking & Langer (1981). A full description of the calculation of the hyperfine structure is presented in Ladd & Fuller (1995).

The DAS $C^{17}O$ $J = 2 \rightarrow 1$ data toward IRS 5 indicate that the $C^{17}O$ has a Gaussian velocity distribution with a FWHM of 0.86 km s^{-1}, consistent with that measured for the $C^{18}O$ line core and in reasonable agreement with the 0.69 km s^{-1} measured in $C^{18}O$ $J = 2 \rightarrow 1$ toward IRS 5 by Menten et al. (1989) using the IRAM 30 m telescope. There is a suggestion, in the residuals of the single-velocity component fit to the $C^{17}O$ $J = 2 \rightarrow 1$ transition, of a second, broader velocity component. The presence of such a component is even more apparent in the fit to the $C^{17}O$ $J = 3 \rightarrow 2$ line. Since this spectrum was taken using the CSO, where the local oscillator is phase-locked, these wings are not the result of variations in the frequency of the local oscillator. A two-velocity component hyperfine fit to this line reduces the rms dispersion of the residuals in region of the line to the same value as in the region of the spectrum without any emission. This fit gives a FWHM for the second component of 2.4 km s^{-1}. The strength of the second component relative to the line peak in the higher lying line, compared to the lower energy transition, suggests that this component arises from relatively warm material.

3.2. *Map Structure*

Maps of the integrated $C^{18}O$ and $C^{17}O$ $J = 2 \rightarrow 1$ emission toward IRS 5 are shown in Figure 2 together with the 730 μm continuum map of the region from Ladd et al. (1995). Both the line-integrated intensity maps and the 730 μm map peak at the location of IRS 5 and trace a very small region around IRS 5. The circle with an area equal to the half-peak contour of the $C^{17}O$ integrated emission has a diameter of 34″. Correcting for the 21″ beam of the JCMT, gives a true size of 27″ or 3800 AU, assuming a distance of 140 pc. The half-peak contour of the $C^{18}O$ integrated emission measured at JCMT traces a region of about the same size. This size scale is significantly smaller than the half-power size of the $C^{18}O$ emission mapped with CSO, which has an extent of 52″ or 7300 AU. This correlation of measured source size with the size of the beam used to make the observations is similar to that seen in continuum observations of young stars (Ladd et al. 1991). This correlation sug-

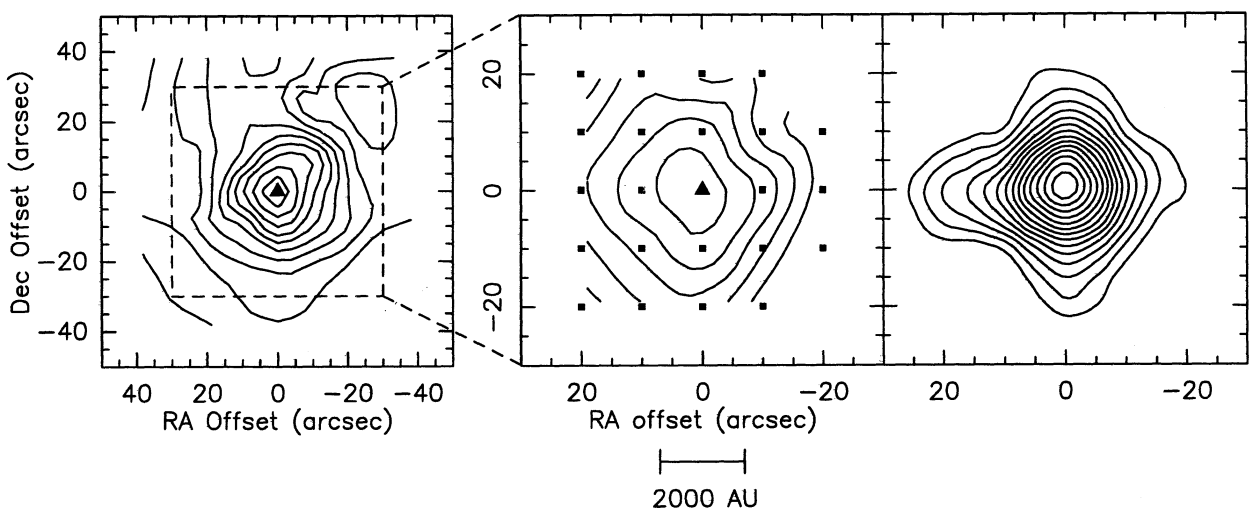

FIG. 2.—Maps of $C^{18}O$ $J = 2 \rightarrow 1$ emission (*left*) and $C^{17}O$ $J = 2 \rightarrow 1$ emission (*center*) integrated over the velocity range 3–9 km s^{-1} and the 730 μm continuum emission (*right*) toward L1551 IRS 5. All the maps were made using the JCMT. The dashed box on the $C^{18}O$ map indicates the region shown in the $C^{17}O$ and continuum maps. All three maps peak at the location of IRS 5 which is indicated by the solid triangle on the CO maps. The scale bar below the $C^{17}O$ map indicates a linear distance of 2000 AU on the $C^{17}O$ and 730 μm maps. The contours for the $C^{18}O$ map start at 1 K km s^{-1} and increase in steps of 0.5 K km s^{-1}. For the $C^{17}O$ map the contour levels start at 0.5 K km s^{-1} and increase in steps of 0.3 K km s^{-1}. The continuum map is contoured starting at 1.5 Jy $beam^{-1}$ with 0.5 Jy $beam^{-1}$ increments between contours.

gests that the underlying distribution does not have a fixed scale size but is consistent with a power-law distribution of emission with projected radius. For comparison, the measured half-peak size of the 730 μm emission is 20″ or 2800 AU. However, it is difficult to compare this size with the size of the molecular line maps as the continuum map has a significant contribution from the central source which is not present in the line maps.

Both line maps in Figure 2 show structure in the extended emission. The $C^{18}O$ has extensions to the south, east, and northwest, while $C^{17}O$ emission has a four lobe structure. The extensions in the $C^{17}O$ to the south and east are similar to those seen in the $C^{18}O$ map. However, the $C^{17}O$ also shows $\sim 10''$ extensions to north and east which are not apparent in the $C^{18}O$ map. The absence of the northern and eastern extensions in the $C^{18}O$ map may be attributable to the higher optical depth in the $C^{18}O$ transition and the presence of significant emission in the wings of the $C^{18}O$ which masks the presence of the extensions (§ 3.3). The four-lobed pattern of the emission in the $C^{17}O$ integrated intensity is very similar in shape to the extended component of the 730 and 850 μm continuum emission (Fig. 2; Ladd et al. 1995). As discussed by Ladd et al., it is unlikely that this structure is due to an instrumental artifact, especially since the $C^{17}O$ and continuum data show similar structures but were taken at different times and with completely different observing techniques.

In order to investigate the nature and origin of this four-lobed structure our analysis of the spectral line maps will concentrate on two components similar to those used discussed by Ladd et al. (1995). These two components will be called the "cross" and "extended" emission. To characterize the material in the cross, the average of the spectra toward the position of IRS 5 and the four positions 10″ north, south, east, and west of IRS 5 will be used. The average of the remaining spectra in the box $\pm 20''$ from IRS 5 will be used to represent the properties of the more extended component of the $C^{17}O$ emission.

It should be noted that the separation of the structure around IRS 5 in to a cross plus extended component is not the only possible model for the emission. For example, it would be possible to model the region as a north–south ridge plus an east–west bar. Such a model might be suggested by the north–south alignment of the radio continuum double detected by Rodríguez et al. (1986) and Beiging & Cohen (1985) and interpreted by Rodríguez et al. as tracing the ionized inner edge of the circumstellar disk around IRS 5. However, the interferometer observations of Sargent et al. (1988) suggest that the dense circumstellar material is not aligned north–south but is at a position angle between 135° and 160° east of north. In addition, the submillimeter spectra of the arms of the cross are not consistent with the presence of a single dust temperature, indicating the presence of at least two different dust components at the location of the arms of the cross (Ladd et al. 1995). A model with a north–south ridge and an east–west bar would therefore require at least two different temperature dust components in the north–south ridge. A cooler component to match the larger scale north–south component (see in the 1100 μm continuum and the $C^{18}O$ line core emission) and a second warmer component at the location of the north and south extensions of the cross to match the 850 μm and 730 μm emission. Since neither the line nor the continuum data show evidence for differences between the north–south extensions of the cross and east–west extensions of the cross, the simplest model is to assume that these extensions arise from similar material, the cross component.

3.3. *Velocity Structure of the Cross and Extended Emission*

The prominence of the cross in the $C^{17}O$ integrated intensity map reflects not only the brighter $C^{17}O$ line toward the cross but also its enhanced line width. The spectrum formed by averaging the central position and the positions 10″ north, east, south, and west (the cross positions) for both CO species are shown in Figure 3. This figure also shows spectra of the extended emission in both CO species. A single velocity component hyperfine fit to the $C^{17}O$ cross spectrum, assuming that the transition is optically thin, indicates the material has a velocity FWHM of 1.32 ± 0.05 km s^{-1} while the extended emission has a FWHM of 1.06 ± 0.06 km s^{-1}. Since the spectrum of the cross is an average of fewer individual spectra than the extended spectrum, it is unlikely that the larger velocity width of the cross is the result of variations in the local oscillator.

The spectra averaged to represent the extended emission are from positions farther from IRS 5 than those representing the cross emission, so it is possible that the width difference between the cross and the extended emission results from a general trend for the regions near IRS 5 to have larger line widths than more distant positions. However, this is probably not the case, as excluding the spectrum toward IRS 5 from the cross spectrum does not significantly change the velocity width. In addition, averaging the four positions (10″, 10″), (−10″, 10″), (−10″, −10″) and (10″, −10″) which are the closest noncross positions to IRS 5, we find a velocity FWHM

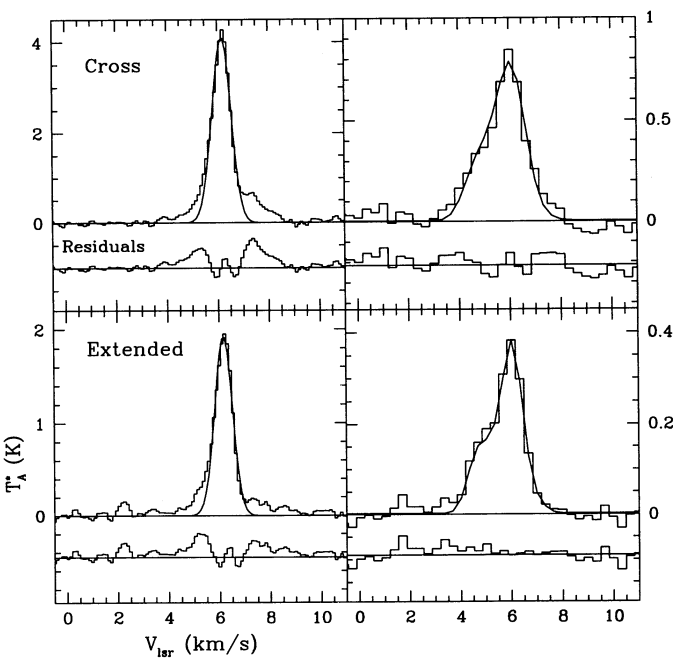

FIG. 3.—The $C^{18}O$ (*left*) and $C^{17}O$ (*right*) $J = 2 \rightarrow 1$ spectra toward the cross and extended material. The cross spectra ($C^{18}O$ upper left, $C^{17}O$ upper right) are the average of the spectra from the (0,0), (10″,0), (−10″,0) (0,10″), (0,−10″) positions in the maps. The extended emission spectra ($C^{18}O$ lower left, $C^{17}O$ lower right) are the average of all the spectra within the box $\pm 20''$ about IRS 5, excluding the cross positions. The solid curves through the spectra are single-velocity component fits. The residuals from this fit to the spectra are shown below each spectrum. The $C^{18}O$ residuals clearly show the presence of a second, broader component. The cross $C^{17}O$ emission residuals are also suggestive of a second component.

of 1.09 ± 0.07, indistinguishable from the value for the spectrum of the extended emission. Again, this difference between the cross and extended emission is not simply the result of the velocity dispersion increasing close to IRS 5.

The $C^{18}O$ $J = 2 \rightarrow 1$ emission from the cross positions (Fig. 3) is clearly not well fitted by a single-velocity component model. Compared to a single component which fits the central spike of emission, the line has additional emission on both the red and blue sides of the line core. The residuals from fitting the $C^{17}O$ $J = 2 \rightarrow 1$ line with a model accounting for the hyperfine structure with a single-velocity component indicate that a single-velocity component fits better than for the $C^{18}O$. However, there is still some slight suggestion in the residuals of the fit for structure similar to that seen in the $C^{18}O$ residuals. The $C^{18}O$ spectrum of the extended emission (Fig. 3) also shows a wing structure of similar shape and intensity relative to the line core as toward the cross positions. The $C^{17}O$ spectrum of the extended material shows no evidence for any wing emission.

3.4. *Line Wing Emission*

Over most of the map the $C^{18}O$ line comprises a narrow central component with excess emission on at least one side of the line. Maps of the $C^{18}O$ emission integrated over three different velocity ranges, corresponding to the blue wing emission, the line core, and the red wing emission, are shown in Figure 4. Although the different velocity components all peak near IRS 5, they have distinctly different spatial distributions. The bulk of the $C^{18}O$ line, the line core emission, traces a region which peaks at the position of IRS 5 and at low intensity levels is elongated north–south. This north–south elongation is similar to that seen at low levels in the 1100 and 1300 μm continuum emission from IRS 5 (Ladd et al. 1995; Mezger, Sievers & Zylka 1991) and also seen in $C^{18}O$ $J = 1 \rightarrow 0$ by Walmsley & Menten (1987) and the $C^{18}O$ $J = 2 \rightarrow 1$ map of Zhou et al. (1994). The blueshifted $C^{18}O$ emission forms an arc around IRS 5 which opens to the southwest and contributes the southern and eastern extensions seen in the integrated intensity map. This arc is similar in shape and location to the shell-like structure seen in the ^{12}CO maps of Moriarty-Schieven & Snell (1988). These authors argue that the shell structure is the edge of the cavity which has been evacuated by the wind from IRS 5.

The redshifted emission arises from a compact elongated ridge of emission passing through the position of IRS 5 at a position angle of about 135° east of north and is responsible for the extension to the northwest in the integrated intensity map. This direction is close to perpendicular to the axis of the large-scale outflow from IRS 5 and is approximately parallel to the $C^{18}O$ $J = 1 \rightarrow 0$ structure observed by Sargent et al. (1988).

Over most of the map the weakness of the $C^{17}O$ line, its hyperfine structure, and the relatively poor spectral resolution of the mapping data make it difficult to determine whether the $C^{17}O$ lines have any wings. However, a second broader component of $C^{17}O$ emission is suggested by the fit to the $C^{17}O$ at the cross positions and the fits to the $C^{17}O$ spectra, especially the $J = 3 \rightarrow 2$ transition, toward IRS 5 (§ 3.1; Fig. 1).

4. ANALYSIS

4.1. *Optical Depth and Excitation Temperature*

The optical depth of the CO transitions was determined from the ratio of the line temperatures of the $C^{17}O$ and $C^{18}O$ $J = 2 \rightarrow 1$ transitions using the method discussed by Myers, Linke, & Benson (1983), modified to account for the hyperfine structure of the $C^{17}O$ transition. A value of 3.5 was adopted for the abundance ratio $C^{18}O/C^{17}O$ (Wilson et al. 1981). The optical depths toward IRS 5 and for the cross and extended components are listed in Table 1. The optical depth of the $C^{17}O$ transition can also be obtained from the ratio of the strengths of the different hyperfine components in the transition. Although the optical depths derived from fitting the hyperfine structure of the $J = 2 \rightarrow 1$ transition are consistent with those derived from the $C^{18}O$ to $C^{17}O$ line ratio, the values are highly uncertain. For example, the hyperfine fit for the cross emission gives an optical depth of 0.9 ± 0.7 and 0.7 ± 0.7 for the extended component. Two factors contribute to this large uncertainty. First, all the components are blended and so the velocity dispersion is not well constrained independent of the other line parameters. Second, the hyperfine ratio poorly constrains the optical depth of nearly optically thin transitions such as the $C^{17}O$ lines toward L1551 IRS 5.

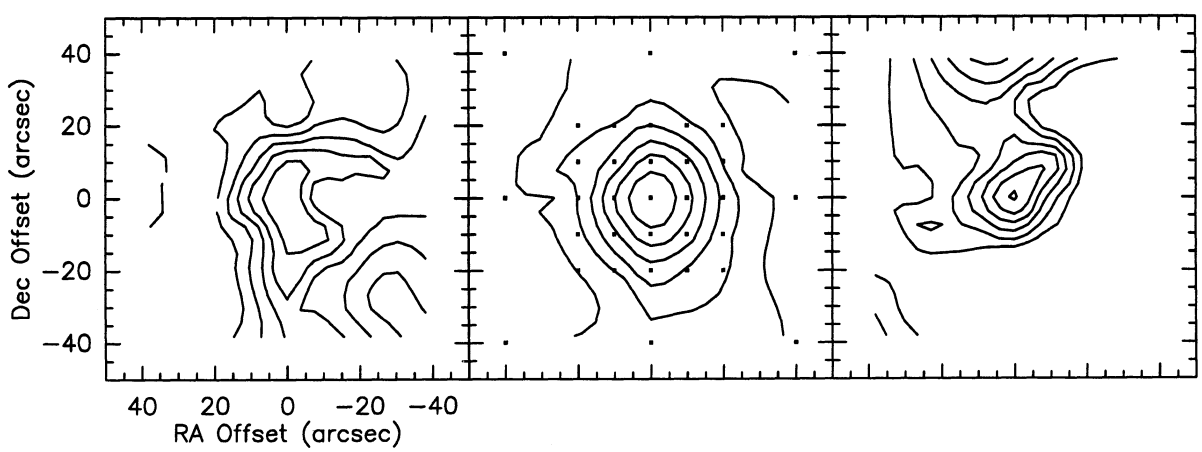

FIG. 4.—The $C^{18}O$ $J = 2 \rightarrow 1$ emission mapped with the JCMT integrated over 4–5.6 km s^{-1} (*left*) corresponding to the blue wing emission, 5.6–6.4 km s^{-1} (*center*) corresponding to the line core and 6.4–9 km s^{-1} (*left*), the red line wing. Each map is centered on IRS 5 and the observed positions are indicated in the center panel. The blueshifted arc of emission is similar to that seen in the ^{12}CO map of Moriarty-Schieven & Snell (1988). The lowest contour levels are 0.12, 0.6, and 0.6 K km s^{-1} with intervals of 0.12, 0.36, and 0.24 K km s^{-1} for the blueshifted, line core, and redshifted emission, respectively.

TABLE 1

PROPERTIES OF THE MATERIAL AROUND L1551 IRS 5

Object	FWHM of $C^{17}O$ (km s^{-1})	$\tau(C^{18}O)$	$\tau(C^{17}O)$	T_{ex} (K)	$N(H_2)$ (10^{22} cm^{-2})	$n(H_2)$ (10^5 cm^{-3})	Mass ($M_\odot$)
IRS 5.....	1.3 ± 0.1	0.6 ± 0.1	0.17 ± 0.03	21 ± 3	2.7	...	...
Cross	1.32 ± 0.05	0.5 ± 0.1	0.14 ± 0.03	20 ± 3	2.2	6	0.11
Extended.....	1.06 ± 0.06	0.7 ± 0.1	0.20 ± 0.03	8 ± 0.5	1.1	2	0.1

NOTES.—The velocity width of the $C^{17}O$ $J = 2 \rightarrow 1$ results from fitting the line profiles assuming the transition is optically thin. The values toward IRS 5 are based on the AOS-C $C^{17}O$ data. The volume density and mass of extended material are calculated using a radius of 20″, corresponding to the size of the region mapped in $C^{17}O$. For the cross emission the measured size of the cross, 27″, has been used.

The excitation temperatures were determined from the line temperature, T_A^*, and the optical depth using a telescope forward efficiency, η_{fss}, of 0.8 (Matthews 1993). A beam filling factor of 0.62, corresponding to the half-maximum size of the emission, 27″, was used in determining the excitation temperature for both the cross component and the measurement toward IRS 5, giving values of 20 and 21 K, respectively. The beam-filling factor for the extended emission was assumed to be unity, giving an excitation temperature of 8 K. The uncertainties given in the table correspond to ± 1 σ changes in the $C^{17}O$ and $C^{18}O$ line peak temperatures.

The largest systematic uncertainty in the excitation temperature probably arises from the choice of the beam-filling factor. The values for the cross component are probably best determined since the cross size, 27″, is reasonably well determined, although if the emission arises from clumps within the beam the excitation temperature could be significantly higher. The magnitude of the uncertainty in the extended emission excitation temperature can be seen by noting that changing the beam-filling factor for the extended component from unity to 0.62, the same as for the cross component, changes only the derived excitation temperature from 7 to 10 K.

An additional source of uncertainty in the optical depths and excitation temperatures arises from the possibility that the velocity widths determined from the AOS-C measurements of the $C^{17}O$ overestimate the true velocity widths (see § 2), Comparing the $C^{18}O$ spectrum toward IRS 5 with the DAS $C^{17}O$ spectrum leads to an optical depth of 1.4 ± 0.1 for the $C^{18}O$ and 0.40 ± 0.03 for the $C^{17}O$. The line strengths then give an excitation temperature of 14 ± 1 K.

An estimate of the temperature of the $C^{17}O$ emitting material toward IRS 5 is also available from the ratio of the CSO $C^{17}O$ $J = 3 \rightarrow 2$ intensity to that of the JCMT $C^{17}O$ $J = 2 \rightarrow 1$. Both the $C^{17}O$ $J = 3 \rightarrow 2$ line and the $J = 2 \rightarrow 1$ line have measured integrated intensities of 1.6 K km s^{-1}. Assuming that the emission in each line has the same size, the major uncertainty in the ratio of intensities is due to the uncertainty in the sideband ratio at the CSO as JCMT and CSO have very similar efficiences at the frequencies of these lines. Estimating an uncertainty in the sideband ratio of 30%, the ratio of integrated intensities implies a temperature of $\gtrsim 25$ K.

The $C^{17}O$ emission has comparable optical depth in the cross and extended material. However, the cross positions have an excitation temperature ~ 20 K, at least a factor of 2 higher than the extended material which has a temperature of ~ 8 K. This excitation temperature difference directly reflects the different observed line brightness in the cross. Given the relatively low critical density of 3×10^4 cm^{-3} for the CO $J = 2 \rightarrow 1$ transitions, these transitions should be thermalized in the dense material near the star (see § 4.2) and so the excitation temperatures are good estimates of the kinetic temperature. Thus the material in the cross is warm with a kinetic temperature of ~ 20 K and the extended material is significantly cooler with a temperature of ~ 8 K. The temperature of the extended component is in reasonable agreement with the ~ 20 K dust temperature expected at ~ 2800 AU from IRS 5 (Kenyon et al. 1993a) and relatively poor coupling between the gas and dust (Ceccarelli, Hollenbach, & Tielens 1995). It should also be noted that evidence for two-temperature components near IRS 5 is not dependent on the cross plus extended component model. The need for two-temperature components results from the decrease in line brightness away from IRS 5 combined with the relatively uniform line optical depth in the region around IRS 5.

4.2. *Column Density, Density, and Mass*

The molecular hydrogen column density toward IRS 5, the cross component, and the extended component are listed in Table 1. The column density was directly estimated from the $C^{17}O$ lines assuming the hydrogen and $C^{17}O$ column density are related through

$$N(H_2) = 1.3 \times 10^7 N(C^{17}O) + 1.4 \times 10^{21} \text{ cm}^{-2} . \quad (1)$$

This relation is based on the $C^{18}O$ column density to visual extinction correlation determined for Heiles' cloud 2 by Cernicharo & Guèlin (1987) assuming a factor of 3.5 for the relative abundance of $C^{18}O$ to $C^{17}O$, and the Bohlin, Savage, & Drake (1978) conversion between hydrogen column density and visual extinction. Adopting the correlation between extinction and $C^{18}O$ column density determined by Frerking, Langer, & Wilson (1982) would increase the derived column densities by $\sim 40\%$.

Toward IRS 5 the $C^{17}O$ emission indicates a column density of 2.7×10^{22} cm^{-2} consistent with both the molecular line observation of Menten et al. (1989) and the recent submillimeter continuum observations of Ladd et al. (1995). Using a radius of 1900 AU for the cross emission, the measured column density of 2.2×10^{22} cm^{-2} and size give a mass of 0.11 $M_\odot$. This is significantly larger than the mass of the cross derived from the continuum emission. However, the $C^{17}O$ mass refers to all the material along the line of sight to the cross whereas the cross mass quoted by Ladd et al., ≤ 0.02 $M_\odot$, refers only to the hot material necessary to match the cross emission and does not include the underlying centrally condensed cold component. Using a radius of 2800 AU for the extended material, corresponding to the 20″ radius of the region mapped, leads to a mass of the extended component of 0.1 $M_\odot$.

The volume density estimated from the column density and estimated source size can also be compared with that predicted

by the model of Butner et al. (1991). Their best-fit model for the far-infrared emission from IRS 5 has a density profile which is consistent with ongoing accretion of core material onto the central star plus disk. This model predicts an average volume density of 9×10^5 cm^{-3} at an angular radius of 13″.8. This is in good agreement with the density of 6×10^5 cm^{-3} estimated here from the $C^{17}O$ observations of the cross. Although the Butner et al. model does not include the effects of the outflow from IRS 5, the densities it predicts may be reasonable estimates if the outflow has not yet significantly altered the radial distribution of the infalling material.

5. DISCUSSION

It is unusual to find a molecular transition which peaks at the position of a young star and traces a compact, but resolved, region around the star. These features of the $C^{17}O$ emission, together with the similarity with the submillimeter continuum maps, demonstrate that, in L1551 IRS 5, the $C^{17}O$ emission predominantely traces the circumstellar material. This is not the case for many other molecules, even when observed with high angular resolution. For example, although NH_3 is a good tracer of the properties of dense cores, it is relatively unusual to find the emission peaking at the location of the stars associated with the cores despite the far-infrared and submillimeter emission from the stars indicating the presence of circumstellar material. In L1551, IRS 5 is located about 20″ from the peak of the NH_3 (1,1) emission (Menten & Walmsley 1985). The reason that the $C^{17}O$ traces such a small region around IRS 5 is that this transition, like the dust continuum emission, has a low optical depth throughout most of the molecular core around IRS 5. Only in the densest regions close to IRS 5 is there a sufficient column density for the $C^{17}O$ to be strong enough to be detectable.

The $C^{17}O$ and 730 and 850 μm continuum emission (Ladd et al. 1995) are very similar in shapes. In addition, analysis of both the line and continuum emission indicates the presence of two components: warm material giving rise to the cross emission, plus a cooler, more spatially extended component. For the cross emission the temperature derived from the $C^{17}O$ $J = 2 \rightarrow 1$ emission, $\sim$20 K, is somewhat lower than the greater than $\sim$50 K suggested by the continuum emission. However, this is not unexpected as the density of the material probed by the $C^{17}O$ is probably not high enough to maintain the gas and the dust at the same temperature (Ceccarelli et al. 1995). It is also important to realize that the analysis of the continuum emission by Ladd et al. (1995) is based on a model comprising a hot dust cross superposed on a cold, centrally condensed dust component. The physical parameters of the two dust components were then estimated by comparing this model with the data. On the other hand, the properties of the $C^{17}O$ emitting material have been determined from the observed spectra, which toward the cross includes a contribution from both the hot cross material and the underlying cold material. Therefore, it is quite reasonable that the temperature of the cross derived from the $C^{17}O$ emission would be lower than estimated from the two-component dust model, and the $C^{17}O$ derived mass of the cross would be much larger than that derived from the continuum emission.

The 1.2 $M_\odot$ of extended, cool material traced by the 1100 μm observations of IRS 5 indicate an average column density of 5×10^{22} cm^{-2} toward the IRS 5 (assuming that the material is distributed spherically around IRS 5 with a density profile which varies with radius r as $r^{-1.5}$). Within a region of projected radius 20″ centered on IRS 5 the continuum observations imply a mass of 0.3 $M_\odot$. Both the column density and mass within the central region are in reasonable agreement with the $C^{17}O$ derived values of 2.7×10^{22} cm^{-2} and a total $C^{17}O$ derived mass of 0.21 $M_\odot$.

This consistency between the continuum and line results support the interpretation that both tracers are indeed tracing the same circumstellar material around IRS 5. The extended component of the $C^{17}O$ emission close to IRS 5 traces the inner region of the extended material traced by the 1100 μm continuum emission (Ladd et al. 1995) and the $C^{18}O$ line core emission (Fig. 4). The similar values of the column densities derived from the line and continuum observations also suggest that there is little evidence for any depletion of $C^{17}O$ in the circumstellar material. Limits on the possible depletion are proportional to the assumed dust absorption coefficient which at 1 mm is estimated to be subject to an uncertainty of between a factor of 2 and 4 (Pollack et al. 1994; Ossenkopf & Henning 1994). Applying the more conservative factor of 4 to the dust column density toward IRS 5 implies that the $C^{17}O$ data are consistent with between a factor of 7 depletion and a factor of 2 overabundance of $C^{17}O$ toward IRS 5 compared to the abundance used above. IRS 5 therefore shows no evidence of the large depletions of CO claimed toward some other young sources (Blake et al. 1995; Mezger et al. 1992).

One difference between the 730 μm map and the $C^{17}O$ emission is the presence of a strong point source component in the 730 μm map which is not obvious in the $C^{17}O$ map. This difference probably results from the difference in optical depth between the line and continuum. After removing the point source contribution from the 730 μm emission (Ladd et al. 1995), the beam-averaged optical depth toward IRS 5 at 730 μm is $\sim$0.04, if a dust temperature of 10 K is adopted (Ladd et al. 1995). Since much of the dust contributing emission along this line of sight is warmer than 10 K, this value is an upper limit to the true optical depth. On the other hand, the beam-averaged optical depth of the $C^{17}O$ is $\sim$0.2–0.3. The smaller optical depth of the continuum emission means that the centrally heated region very close to IRS 5 is much more apparent in the continuum emission than in the line emission.

5.1. *Origin of the Structure*

The $C^{17}O$ emission traces two different components: a bright cross of emission plus a more distributed component. As described above, the cross emission has both a higher excitation temperature and a larger velocity dispersion than the extended emission. Both these differences would naturally arise if the cross emission traces a region of interaction between the outflow from IRS 5 and dense circumstellar gas.

Comparison of the cross and blueshifted $C^{18}O$ emission with the ^{12}CO outflow map of Moriarty-Schieven & Snell (1988) suggests that the arms of the cross trace the walls of the cavity cleared by the outflow sweeping up the circumstellar material. The ^{12}CO maps show that close to IRS 5 both the blue and red outflow lobes have opening angles consistent with the edges of the outflow cavity being aligned approximately north–south and east–west. As shown in Figure 5 of Ladd et al. (1995), the 730 μm continuum emission, which is similar in shape to the $C^{17}O$ emission (Fig. 2), traces the outer edge of the cavity seen in ^{12}CO. At a much smaller size scale, high-resolution near-infrared and optical images of IRS 5 also provide evidence that the outflow cavity has a large opening angle. Images at i and K band (Campbell et al. 1988; Hodapp

et al. 1988) both show nebulae in the blue shifted outflow lobe which have opening angles $\sim 120°$ within a few arcseconds of IRS 5.

Dynamically, the observed motions of the cross material are consistent with an interaction between dense gas and the outflow. Even if the whole line width of the $C^{17}O$ cross material were the result of the action of the outflow, the momentum in the $C^{17}O$ motions, 0.07 $M_\odot$ km s^{-1}, is a small fraction of the momentum in the outflow close to IRS 5, 16 $M_\odot$ km s^{-1} (Moriarty-Schieven & Snell 1988).

Evidence that the cross material is tracing the edge of the outflow cavity rather than the axis of the outflow from IRS 5 or two unrelated components of material, one east–west and the other north–south, also comes from considering the location of the eastern side of the radio continuum jet from IRS 5. Within 2″ of the north–south aligned radio double system which comprise IRS 5 (Bieging & Cohen 1985; Rodríguez et al. 1986), the radio continuum jet is elongated in a direction $\sim 70°$ east of north (Fig. 5). However, the position angle of the jet changes with increasing distance from the central double. At 10″ from the central source, the eastern side of the jet has a position angle 60° east of north, more nearly aligned with the axis of the large-scale outflow from IRS 5 (Snell et al. 1985). If the jet maintains or increases its position angle to the $\sim 20''$ size scale studied here, the radio jet would fall between the northern and eastern arms of the cross. The western side of the jet has a similar axis to the eastern jet at $\sim 2''$ from IRS 5, but at 10″ the western side of the jet is not as extended as the eastern side and points nearly due south of IRS 5. Further evidence supporting the model of the arms of the cross as the edges of the outflow cavity comes from the high-resolution observations of IRS 5 by Sargent et al. (1988) who identified a ~ 700 AU long, high-density region traced by $C^{18}O$ centered on IRS 5. This material has a position angle of 135° to 160° east of north and is aligned between the arms of the cross and perpendicular to the radio jet. Sargent et al. found little evidence of dense material aligned north–south as would be suggested by the Rodríguez et al. (1986) model for the central radio double as the ionized inner edge of the circumstellar disk. More recent higher angular resolution observations have resolved one axis of the circumstellar disk (Lay et al. 1994) showing it to have a 60 AU semimajor axis at a position angle consistent with that measured by Sargent et al.

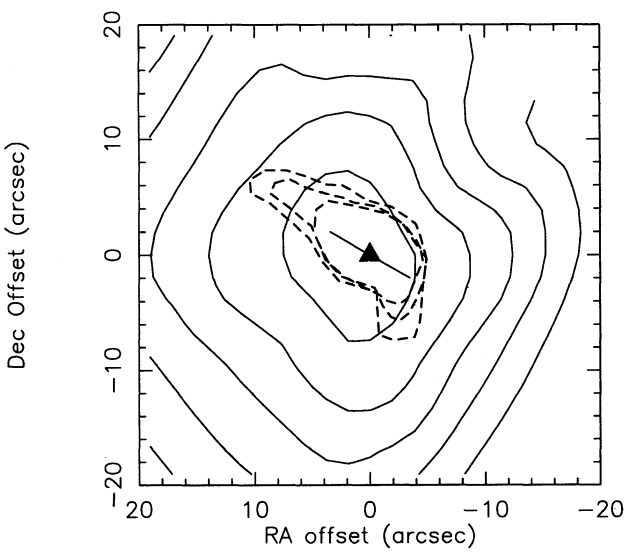

FIG. 5.—Comparison of the 5 GHz radio continuum emission from IRS 5 and the integrated $C^{17}O$ emission. The solid contours show the integrated $C^{17}O$ $J = 2 \rightarrow 1$ emission measured at the JCMT. The contour levels are the same as in Fig. 2. The solid triangle marks the location of IRS 5. The dashed contours show the 5 GHz radio continuum jet mapped by Snell et al. (1985). The contour levels shown are 0.2, 0.3 and 0.4 mJy beam^{-1}. Note that the northeastern lobe of the jet passes between the northern and eastern arms of the $C^{17}O$ cross. The solid line passing through the location of IRS 5 shows the position angle of the jet as mapped at 5 GHz at higher angular resolution by Bieging, Cohen, & Schwartz (1984). The length of the line is about twice the length of the jet in the high-resolution map.

If the cross emission is tracing material which has been heated and disturbed by the outflow, the extended material provides the best estimate for velocity dispersion of the undisturbed core material. However, it is possible that even in the extended material some of the velocity dispersion is due to interaction with the outflow and so the virial mass estimate provides only an upper limit to the true mass. Correcting for the velocity resolution of the JCMT system, the extended material has a velocity FWHM of 1.0 km s^{-1}. This leads to a FWHM velocity for the molecular hydrogen, assuming a temperature of 8 K, of 1.1 km s^{-1}. Adopting a radius of 2800 AU, consistent with the size of region mapped in $C^{17}O$, this corresponds to a virial mass of between 2 and 3 $M_\odot$, depending on the mass distribution at smaller size scales.

However, the absolute velocity width of the $C^{17}O$ lines, and hence the virial mass, is significantly affected by the poor spectral resolution of AOS-C (see § 2). If the extended component has a line width as narrow as ~ 0.8 km s^{-1} as seen in the DAS observations and confirmed by Ladd & Fuller (1995), the range of virial masses drops to 1–1.6 $M_\odot$. Even the lower limit of this mass range is significantly in excess of the mass determined from the analysis of the $C^{17}O$ spectra. However, modeling and observations suggest that the star plus disk have a mass between 0.5 and 1 $M_\odot$ (Ladd et al. 1991; Keene & Masson 1990), so the virial mass is consistent with the mass of the gas plus the mass of the central star and disk. The $C^{17}O$ is therefore tracing a region in the molecular material around IRS 5 where the gravitational field is dominated, not by the mass of gas and dust, but rather by the central young star. It is in such regions that evidence for continuing accretion onto the young star might be expected to be found.

5.2. *The Mass Accretion Rate near IRS 5*

Perhaps the most successful model for the collapse of dense cores to form young stars has been the inside-out collapse of a singular isothermal core modeled by Shu (1977) and Terebey et al. (1984). In this model the inner region of a core collapses first and an expansion wave propagates outward at the local signal speed. The radius of the expansion wave, r_{exp}, at a time t after the start of the core collapse is then at, where a is the isothermal sound speed given by $a^2 = kT/m$ with T the kinetic temperature, m the mean molecular mass, and k Boltzmann's constant.

It is difficult to determine the age of embedded young stars such as L1551 IRS 5, but one estimate of the minimum age can be obtained from the dynamical age of the outflow, since outflows are thought to start very soon after the formation of the star (Terebey, Vogel, & Myers 1989). For the L1551 IRS 5 outflow, Moriarty-Schieven & Snell (1988) find an age of between 3×10^4 yr and 10^5 yr. This range is consistent with that found by Kenyon et al. (1993a) from modeling the spectral energy distribution of IRS 5. Adopting an isothermal sound speed of 0.19 km s^{-1}, corresponding to 10 K molecular hydro-

gen with 10% helium, this range in ages corresponds to a present-day radius of the expansion wave of between 1200 and 3900 AU (or between 8″ and 28″). Thus some, and possibly all, the region traced by $C^{17}O$ should have already passed through the expansion wave and be collapsing toward IRS 5.

Using the measured size, density, and velocity dispersion it is possible to place an upper limit on the mass accretion rate, $\dot{M}$, on the IRS 5 through the relation

$$\dot{M} = 4\pi r^2 mn v_{\rm infall} . \quad (2)$$

Adopting a radius r corresponding to 20″, a number density n of 2×10^5 cm^{-3}, and an infall velocity, $v_{\rm infall}$ of 0.55 km s^{-1}, corresponding to accretion at half the FWHM velocity for the molecule of mean mass, m, inferred from the observed velocity FWHM of the $C^{17}O$, leads to an accretion rate of 1.4×10^{-5} $M_\odot$ yr^{-1}. This is an upper limit to the true mass accretion rate at the size scale of the $C^{17}O$ core as the $C^{17}O$ lines do not show any velocity shifts indicative of accretion velocities as large as adopted. In addition, it is likely that even for the extended material some fraction of the observed line width is due to interaction with the outflow from IRS 5.

It is interesting to note that this upper limit to the mass accretion rate implied by the extended $C^{17}O$ material is only a factor of 1–3 larger than that estimated by Kenyon et al. (1993b) from modeling the scattered light nebula associated with IRS 5. On the other hand, it is also interesting to note that the mass *outflow* rate in the outflow within ~15″ of IRS 5 is estimated to be in the range of 10^{-4} $M_\odot$ yr^{-1} to 10^{-5} $M_\odot$ yr^{-1} (Fridlund & Knee 1993), consistent with values for the whole outflow (Moriarty-Schieven & Snell 1988). Thus it is possible that within ~15″ of IRS 5 a larger mass of material is currently being ejected than is infalling into the central region around IRS 5. That the mass outflow rate is larger than the infall rate at these radii must indicate either that the final mass of IRS 5 will be no more than the total mass currently within 15″ to 20″ of IRS 5, or that the time-averaged mass outflow rate at these size scales is smaller than currently observed. This later possibility is consistent with the interpretation that IRS 5 is currently in an FU Orionis type outburst phase, during which it has a mass outflow rate higher than the average during its protostellar evolution. Evidence from optical and infrared spectra that IRS 5 is in such an outburst has been presented by Mundt et al. (1985), Carr, Harvey, & Lester (1987), and Stocke et al. (1988). It is believed that FU Ori events are powered by high accretion rates through the circumstellar disks around young stars (Hartmann & Kenyon 1985). However, this high disk accretion rate results from the release of material previously stored in the disk and therefore is not necessarily associated with high-mass accretion rates through the more extended circumstellar region.

5.3. *Evolutionary Status of L1551 IRS 5*

The spectral energy distribution of L1551 IRS 5 (Ladd et al. 1991) and the bolometric temperature derived from it, 97 K (Chen et al. 1995), indicate that this source is one of the youngest sources in Taurus. Chen et al. identified only two sources in Taurus younger than IRS 5, L1527 (IRAS 04368 + 2557) and L1551 NE which have bolometric temperatures of 59 K and 75 K, respectively. The $L_{\rm submm}/L_{\rm bol}$ age indicator (André, Ward-Thompson, & Barsony 1993) suggests that IRS 5 is somewhat more evolved but is still a relatively young class I source (Lada 1987). The bolometric temperature of IRS 5 indicates an age of 1.1×10^4 yr (with a 1 σ uncertainty of a factor of 3) which, within the rather large uncertainty, is in reasonable agreement with the ages estimated from the outflow (Moriarty-Schieven & Snell 1988; Bachiller, Tafalla, & Cernicharo 1994) and modeling of its spectral energy distribution (Kenyon et al. 1993a), 3×10^4 yr to 10^5 yr.

IRS 5 is the most luminous embedded source in Taurus (Kenyon et al. 1993a). As discussed above (§ 5.2), its high luminosity may be due to it currently undergoing an FU Ori outburst; however, it is also possible that IRS 5 is a more massive star than the 0.5 $M_\odot$ typical of Taurus (Kenyon et al. 1993a). The relatively large virial mass estimated from the observations could be consistent with this possibility, but the virial mass may overestimate the true mass as it is possible that even in the extended component of the $C^{17}O$ emission some of the velocity dispersion is due to the outflow.

Despite its young age, the $C^{17}O$ and $C^{18}O$ results presented here show a significant amount of the circumstellar emission in these lines arises from material close to the star which has been disturbed by the outflow. There is, however, evidence of more quiescent circumstellar material which is presumably less affected by the outflow and therefore provides the best chance to study the pristine circumstellar material. This quiescent material is best traced by the extended component of the $C^{17}O$ emission but is poorly traced by the $C^{18}O$ emission close to IRS 5.

The presence of both quiescent and disturbed circumstellar material close to IRS 5 and the absence of net accretion into the central region containing the young star suggests that L1551 IRS 5 is in a transitional stage between younger sources, which have larger amounts of circumstellar material and more highly collimated outflows and more evolved sources with less circumstellar material (Ladd & Fuller 1995).

6. CONCLUSIONS

1. New observations of the $J = 2 \rightarrow 1$ transitions of $C^{18}O$ and $C^{17}O$ show that these lines trace a very small region around the embedded young star L1551 IRS 5. At the resolution of these observations, both transitions peak at the location of IRS 5 and the half-power radius of material traced by the transitions is ~1900 AU.

2. $C^{17}O$ traces two components around IRS 5. The brighter component has a four-lobed, crosslike distribution and is very similar in size and shape to the 850 μm and 730 μm emission from IRS 5 mapped by Ladd et al. (1995). The cross emission is warmer, brighter, more compact and has a larger velocity dispersion than the extended, second component. The interpretation of a warm cross of material overlying a cooler more extended component is consistent with the model for the submillimeter continuum emission by Ladd et al. (1995).

3. The higher temperature and larger line width of the cross component, and the cross geometry when compared with maps of the CO outflow and radio continuum jet close to IRS 5, all suggest that the cross emission traces the edges of the cavity cleared by the outflow.

4. The $C^{18}O$ emission has significant line wings which trace distinct components of the circumstellar region around IRS 5. At least one of the wing components is clearly associated with the outflow cavity seen in ^{12}CO observations. The other component extends to the northwest of IRS 5.

5. The $C^{17}O$ probes a region of the core associated with IRS 5 in which the central young star contributes a significant fraction of the gravitational field. It is in such regions that evidence

of infall should be detectable. However, much of the molecular emission from this region, the cross emission, is from material disturbed by the outflow. If such regions of interaction are common close to young stars, they will significantly complicate searches for signatures of the infall of material.

6. The observed properties of the extended $C^{17}O$ material lead to an upper limit for the mass accretion rate on to the young star IRS 5 of $1.4 \times 10^{-5}\ M_{\odot}\ yr^{-1}$. This value is comparable with other estimates for the mass accretion rate but is also comparable to, or lower than, the measured mass outflow rate close to IRS 5.

G. A. F. acknowledges the support of a NRAO Jansky Fellowship. G. A. F. would like to thank the Laboratory for Millimeter Wave Astronomy at the University of Maryland for their hospitality while writing parts of this paper. E. F. L. acknowledges the support of the James Clerk Maxwell Telescope Fellowship. F. C. A. is supported by NASA grant NAGW-2802, an NSF Young Investigator Award, and by funds from the Physics Department at the University of Michigan. We thank the anonymous referee for several helpful comments.

REFERENCES

Adams, F. C., Lada, C. J., & Shu, F. H. 1987, ApJ, 312, 788
André, P., Ward-Thompson, D., & Barsony, M. 1993, ApJ, 406, 122
Bachiller, R., Tafalla, M., & Cernicharo, J. 1994, ApJ, 425, L93
Biechman, C. A., et al. 1986, ApJ, 307, 337
Bieging, J. H., & Cohen, M. 1985, ApJ, 289, L5
Bieging, J. H., Cohen, M., & Schwartz, R. D. 1984, ApJ, 287, 69
Blake, G. A., Sandell, G., van Dishoeck, E. F., Groesbeck, T. D., Mundy, L. G., & Aspin, C. 1995, ApJ, 441, 689
Bohlin, R. C., Savage, B. D., & Drake, J. F. 1978, ApJ, 224, 132
Butner, H. M., Evans, N. J., Lester, D. F., Leverault, R. M., & Strom, S. E. 1991, ApJ, 376, 636
Cabrit, S., & Andre, P. 1991, ApJ, 379, L25
Campbell, B., Persson, S. E., Strom, S. E., & Grasdalen, G. L. 1988, AJ, 95, 1173
Carr, J. S., Harvey, P. M., & Lester, D. 1987, ApJ, 321, L71
Ceccarelli, C., Hollenbach, D., & Tielens, A. G. G. M. 1995, in preparation
Cernicharo, J., & Guèlin, M. 1987, A&A, 176, 299
Chen, H., Myers, P. C., Ladd, E. F., & Wood, D. O. S. 1995, ApJ, 445, 377
Cohen, M., Harvey, P. M., Schwartz, R. D., & Wilking, B. A. 1984, ApJ, 278, 671
Elias, J. 1978, ApJ, 224, 857
Frerking, M. A., & Langer, W. D. 1981, J. Chem. Phys., 74, 6990
Frerking, M. A., Langer, W. D., & Wilson, R. W. 1982, ApJ, 262, 590
Fridlund, C. V. M., & Knee, L. B. G. 1993, A&A, 268, 245
Fuller, G. A. 1993, in Graduate Workshop On Star Formation, ed. J.-P. Arcoragi, P. Bastien, & R. Pudritz (Univ. de Montréal: Département de Physique)
Fuller, G. A., & Myers, P. C. 1993, ApJ, 418, 273
Hartmann, L., & Kenyon, S. J. 1985, ApJ, 299, 462
Hodapp, K. W., Capps, R., Strom, S. E., Salas, L., & Grasdalen, G. L. 1988, ApJ, 335, 814
Keene, J., & Masson, C. R. 1990, ApJ, 355, 635
Kenyon, S. J., Calvet, N., & Hartmann, L. 1993a, ApJ, 414, 676
Kenyon, S. J., Whitney, B. A., Gomez, M., & Hartmann, L. 1993b, ApJ, 414, 773
Lada, C. J. 1987, in IAU Symp. 115, Star Forming Regions, ed. M. Peimbert & J. Jugaku (Dordrecht: Kluwer), 1
Ladd, E. F., Adams, F. C., Casey, S., Davidson, J. A., Fuller, G. A., Harper, D. A., Myers, P. C., & Padman, R. 1991, ApJ, 366, 203
Ladd, E. F., & Fuller, G. A. 1995, ApJ submitted
Ladd, E. F., Fuller, G. A., Padman, R., Myers, P. C., & Adams, F. C. 1995, ApJ, 439, 771
Lay, O. P., Carlstrom, J. E., Hills, R. E., & Phillips, T. G. 1994, ApJ, 434, L78
Matthews, H. E. 1993, The James Clerk Maxwell Telescope: A Guide for the Prospective User (Hilo: Joint Astronomy Centre)
Menten, K. M., Harju, J., Olano, C. A., & Walmsley, C. M. 1989, A&A, 223, 258
Menten, K. M., & Walmsley, C. M. 1985, A&A, 146, 369
Mezger, P. G., Sievers, A. W., Haslam, C. G. T., Kreysa, E., Lemke, R., Mauersberger, R., & Wilson, T. L. 1992, A&A, 256, 631
Mezger, P. G., Sievers, A., & Zylka, R. 1991, in IAU Symp. 147, Fragmentation of Molecular Clouds and Star Formation, ed. E. Falgarone, F. Boulanger, & G. Duvert (Dordrecht: Kluwer), 245
Moriarty-Schieven, G. H., & Snell, R. L. 1988, ApJ, 332, 364
Mundt, R., Stocke, J., Strom, S. E., Strom, K. M., & Anderson, E. R. 1985, ApJ, 297, L41
Myers, P. C. 1994, in The Structure and Content of Molecular Clouds, ed. T. L. Wilson & K. J. Johnston (Berlin: Springer), 207
Myers, P. C., Fuller, G. A., Mathieu, Beichman, C. A., Benson, P. J., Schild, R. E., & Emerson, J. P. 1987, ApJ, 319, 340
Myers, P. C., Linke, R., & Benson, P. J. 1983, ApJ, 264, 517
Ossenkopf, V., & Henning, T. 1994, A&A, 291, 943
Parker, N. D., Padman, R., & Scott, P. F. 1991, MNRAS, 252, 442
Pollack, J. B., Hollenbach, D., Beckwith, S., Simonelli, D. P., Roush, T., & Fong, W. 1994, ApJ, 421, 615
Rodríguez, L. F., Cantó, J., Torrelles, J. M., & Ho, P. T. P. 1986, ApJ, 301, L25
Sargent, A. I., Beckwith, S., Keen, J., & Masson, C. R. 1988, ApJ, 333, 936
Shu, F. H. 1977, ApJ, 218, 488
Snell, R. L., Bally, J., Strom, S. E., & Strom, K. M. 1985, ApJ, 290, 587
Snell, R. L., Loren, R. B., & Plambeck, R. L. 1980, ApJ, 239, L17
Stocke, J. T., Hartigan, P. M., Strom, S. E., Strom, K. M., Anderson, E. R., Hartman, L., & Kenyon, S. J. 1988, ApJS, 68, 229
Strom, S. E., Strom, K. M., & Vbra, F. J. 1976, AJ, 81, 320
Terebey, S., Chandler, C. J., & Andrè, P. 1983, ApJ, 414, 759
Terebey, S., Shu, F. H., & Cassen, P. 1984, ApJ, 286, 529
Terebey, S., Vogel, S. N., & Myers, P. C. 1989, ApJ, 340, 472
Walmsley, C. M., & Menten, K. M. 1987, A&A, 179, 231
Wilson, R. W., Langer, W. D., & Goldsmith, P. F. 1981, ApJ, 243, L47
Zhou, S., Evans, N. J., Wany, Y., Peng, R., & Lo, K. Y. 1994, ApJ, 433, 131